13th International Symposium on Particle Image Velocimetry – ISPIV 2019
Munich, Germany, July 22-24, 2019

Study of convective heat transfer in an impinging swirling jet by time-resolved PLIF/IR thermometry and stereo PIV

Dmitriy Sharaborin[1,2], Sayan Protasov[1,2], Dmitriy Markovich[1,2]*,

Vladimir Dulin[1,2]

[1]Kutateladze Institute of Thermophysics, Siberian Branch of the Russian Academy of Sciences, Novosibirsk, Russia

[2] Novosibirsk State University, Novosibirsk, Russia

* dmark@itp.nsc.ru

Abstract

The present paper reports on a combined application of time-resolved stereoscopic particle image velocimetry (PIV) and planar laser-induced fluorescence (PLIF) methods to measure flow and temperature fields in a submerged swirling water jet, impinged normally on a flat heated surface. Simultaneously, the impingement surface temperature was monitored via high-speed IR-imaging. A multi-frame PIV algorithm was used to process the PIV images. A number of image filtering routines, including spatial and temporal filtering, was necessary to obtain a reliable accuracy of the temperature evaluation from the PLIF snapshots. Difference between the temperature of the liquid in vicinity of the wall and wall temperature, evaluated correspondingly from the PLIF and IR imaging, is found to be below 1°C.

1 Introduction

Jet flows impinging on flat surfaces are relevant for a number of technical applications, including cooling, heating, coating, etc. Some of the applications assume uniform heat and mass transfer. Others require achievement of the highest possible local transfer rates. One of the options to intensify convective transfer in impinging jets is the organization of flow swirl, which causes broadening of the jet and increases radial and tangential velocity components. Besides, breakdown of the swirling jet's vortex core occurs for high enough swirl rates and dramatically intensifies transport and mixing near the nozzle exit. On the other hand, strong swirl results in formation a recirculation zone in the jet core, which may reduce local heat transfer near walls due to the flow stagnation.

Huang and El-Genk (1998) have studied effect of the flow swirl on heat transfer from impinging surface and shown that it significantly affects the local heat transfer. The measurements of heat transfer were reported but the flow structure analysis was limited by visualization. Volchkov et al. (1996) have also outlined a reduction of the heat transfer from the surface with increase of the swirl for the distances of several nozzle diameters. However, for distances less than two nozzle diameters the flow swirl sufficiently increased heat transfer.

Azevedo et al. (1997) have investigated effect of the flow swirl on the distribution of mass transfer coefficient for impinging jet with the Reynolds number in the range from 9 000 to 45 000 by using method of naphthalene sublimation. For the separation distances between the wall and nozzle of 2-8 diameters, they have found reduction of the mass transfer with increase of the swirl rate. Abrantes and Azevedo (2006) have conducted velocity measurements in a swirling impinging jet at Re = 21 000 by using PIV and laser Doppler anemometry. The have confirmed that the flow swirl can significantly increase heat transfer from the surface for small separation distances (viz., for quarter of the nozzle diameter). IR imaging is an efficient technique to perform wall temperature measurements for this purpose with sufficient spatial and temporal resolution (Carlomagno and Cardone 2010). In particular, IR thermometry was successful used for the temperature measurements in swirling impinging jets by Ianiro and Cardone (2011).

It is important that swirling jets are often featured by unsteady flow dynamics, corresponding to precession of the jet's vortex core, which becomes very intensive in turbulent jets with strong swirl and vortex breakdown. This unsteady flow feature in impinging swirling jets is studied insufficiently, especially its contribution to the heat transfer. Better understanding of the swirl effect on the flow structure and heat transfer in swirling jets requires measurements of the instantaneous velocity and temperature fields. Nozaki et al. (2003) have analyzed convective heat transfer in the wall region of a swirling impinging jet at Re = 4 000 for separation distance between the nozzle and wall of two nozzle diameters. The authors have combined PIV with PLIF (planar laser-induced fluorescence) method for the simultaneous measurements of the instantaneous velocity and temperature fields in the turbulent flow. They have shown that formation of the central recirculation zone in impinging jet with swirl reduces heat transfer from the wall surface.

The aim of the present paper is to investigate experimentally dynamics of flow and temperature fields in an impinging jet flow under conditions of high swirl and vortex core breakdown. The study is performed by a combined application of time-resolved stereoscopic PIV and PLIF systems. Besides, the wall temperature is monitored via IR-thermography (similar to, for example, Astarita et al. 2000, Carlomagno and Cardone 2010).

2 Experimental setup

The experiments were performed for a closed hydrodynamic circuit, included a test section made of plexiglass, water pump, overflow tank with heat exchanger, piping system and flow meter. Temperature of the circulating water was controlled by thermal resistance transducers, installed in the test section and water tank. During the experiments, the temperature of the water was kept constant at 25 °C with accuracy of 0.2 °C. The jet flow, organized by a contraction nozzle (with the outlet diameter of d = 15 mm), impinged normally on a flat surface made of a sapphire glass (4 mm thick, 150×150 mm in size) and heated by an electric current. On the water side the sapphire glass was coated by a thin conductive film (1.2 μm thick) of indium-tin oxide (ITO, solid phase $(In_2O_2)_{0.9}$-$SnO_2)_{0.1}$) transparent in the visible range. The electric current of 16 A passed through the coating, providing a uniform heating of 3.6 W/cm^2. A Titanium HD 570M (FLIR Systems ATS) IR-camera with a spectral range of 3.7-4.8 μm recorded the temperature of the conductive film on the heating element, which varied from 27°C to 38°C.

A vane swirler was mounted inside the nozzle to produce jet with an angular momentum (as in Alekseenko et al., 2007). Using swirlers with different inclination angles of vanes, jets with different

swirl rates (defined as the ratio of the jet angular momentum flux and the axial momentum flux, normalized by the nozzle exit radius) could be produced. The swirl rates were estimated based on the geometrical parameters of the swirlers (Gupta et al. 1984):

$$S = \frac{2}{3}\left(\frac{1-\left(d_1/d_2\right)^3}{1-\left(d_1/d_2\right)^2}\right)\tan\left(\psi\right) \quad (1)$$

Here d_1 = 7 mm is the diameter of the centerbody supporting the vanes, d_2 = 27 mm is the external diameter of the swirler, and ψ=55° is the vanes inclination angle relatively to the axis. In the present study the swirl rate was S = 1.0, whereas the critical value for a vortex breakdown (in a free jet flow configuration) and formation of a recirculation zone was approximately 0.6. The Reynolds number, defined on the basis of the jets's bulk velocity, nozzle exit diameter and kinematic viscosity of the fluid, was fixed as Re = $U_0 d/\nu$ = 5 000. In the present study the nozzle-to-plate distance H was equal to 1d.

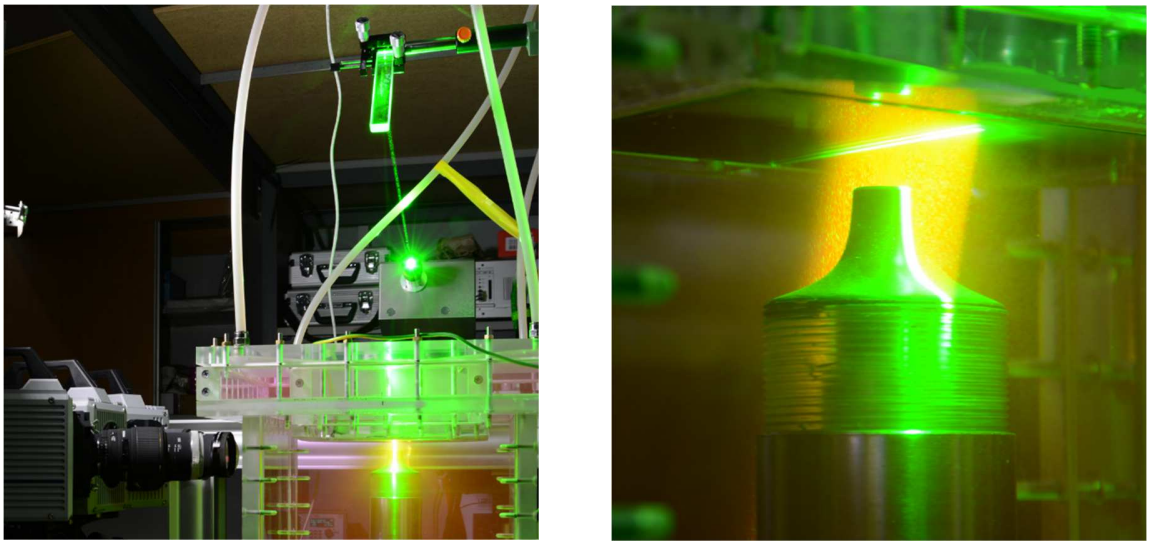

(a) PIV/PLIF system (b) Nozzle and flow illumination

Figure 1: Photographs of experimental setup.

The PIV/PLIF system (Figure 1) consisted of a Photonics DM high-repetition pulsed Nd:YAG laser (150 ns pulses with energy up to 8 mJ at a repetition rate of 10 kHz) and three Photon SA5 high-speed CMOS cameras (with 7.5 kHz rate of full frames with 1024×1024 pixel size and dynamic range of 12 bit). 20-μm polyamide tracer particles with minimal buoyancy were added to the water to provide PIV measurements. The PIV cameras were equipped with narrow band-pass filters with approximately 80% transmittance in the range of 532 ±5 nm. For the PLIF measurements, Rhodamine B fluorescent dye was solved in the water. The PLIF camera was equipped with a long-pass optical filter, which blocked radiation with wavelength less than 560 nm. The cameras and laser were synchronized by using a TTL signal generator BNC 575 by Berkeley Nucleonics. The acquisition rate was 3.5 kHz. 5500 images were recorded during two independent runs.

3 Data processing

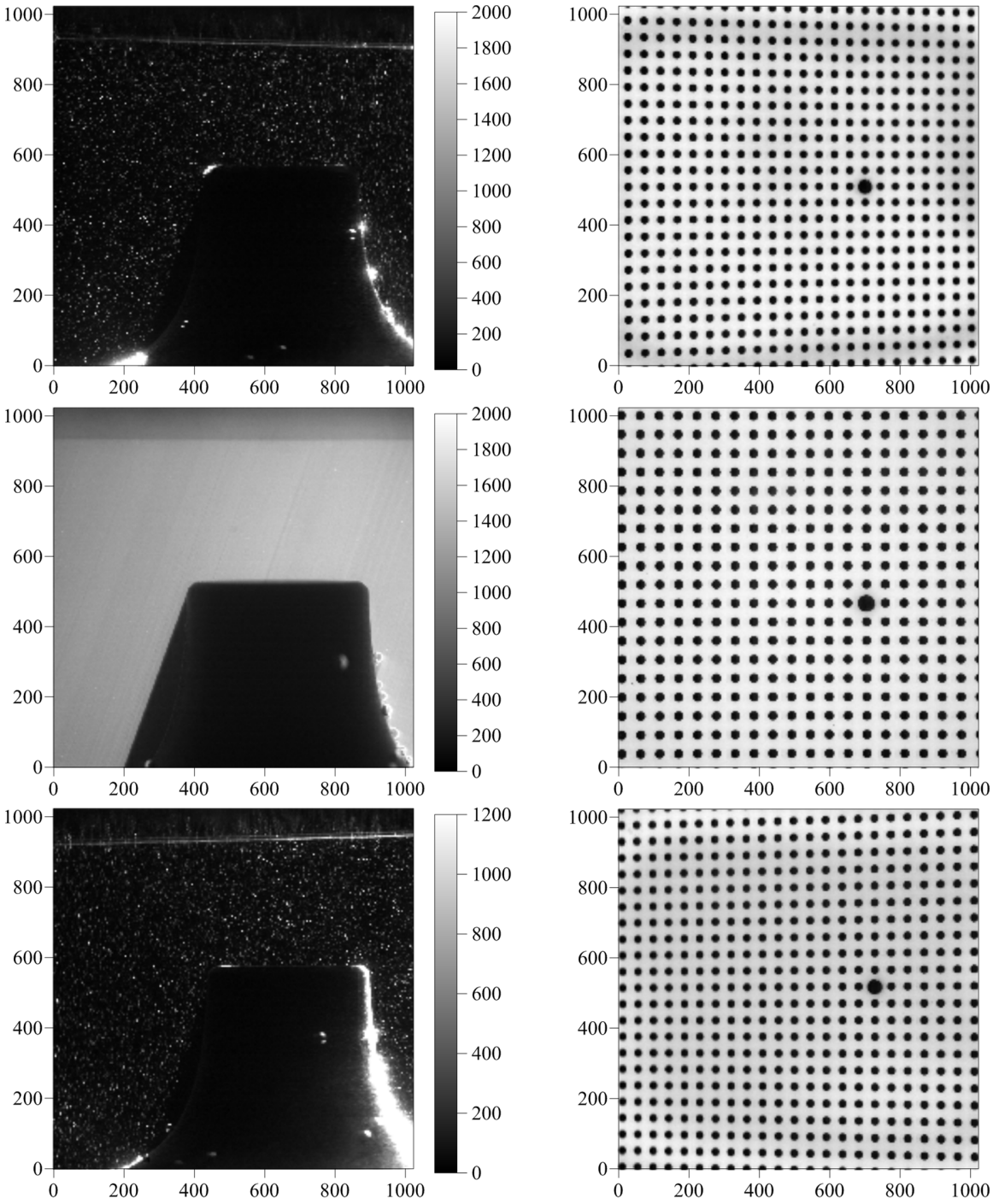

Figure 2: Examples of PIV and PLIF images.

An in-house "ActualFlow" software, developed in the Institute of Thermophysics, was used to acquire and process the PIV and PLIF data. Spatial calibration of the PIV/PLIF cameras was performed by using a planar calibration target (100×100 mm) and third-order polynomial transforms (Soloff et al. 1997). Raw PIV and PLIF images, including those of the calibration target, are shown in Figure 2. The particles displacement was evaluated by using a multi-frame pyramid correlation algorithm (similar to that of Sciacchitano et al. 2012). Final size of the interrogation windows was 16×16 pixels. The spatial overlap factor of the windows was set to 50%.

The PLIF system was calibrated by imaging local variation of the fluorescence yield with the temperature in the range of 24°C to 30°C. This was performed by uniformly heating the water solution of Rhodamine B in the entire test section prior and after the series of the experiments. Examples of the calibration PLIF images are shown in Figure 3. The temperature calibration was obtained by averaging the PLIF intensity over a region of interest between the nozzle and the impingement surface. Variation of the spatially averaged intensity with the temperature is shown in Figure 4. For the considered range of temperatures (6°C) the intensity variation is approximately 14%.

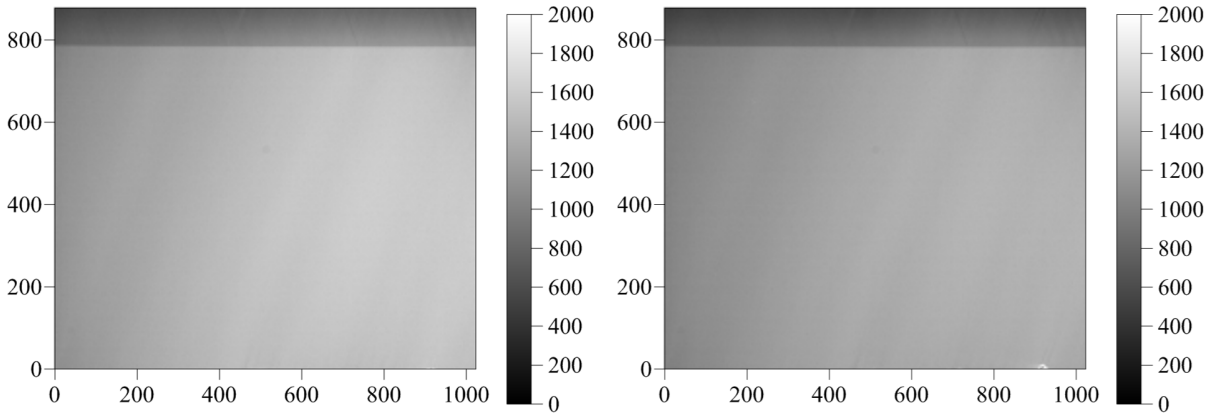

Figure 3: Temperature calibration images for PLIF method.

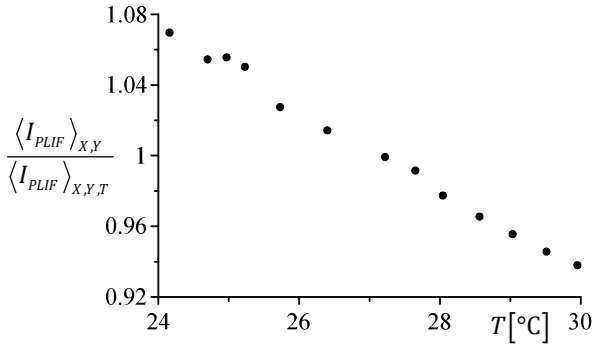

Figure 4: Variation of intensity in a region of interest depending on liquid temperature.

During the PIV/PLIF experiments, when the impingement surface was heated by the electric current, the laser light was refracted due to a non-uniform temperature gradient near the wall. Therefore, the

PLIF images contained a number of bright and dark stripes. Besides, the PLIF images included noise from the CMOS sensor and some remaining images of the tracer particles. In order to remove these artifacts and improve signal-to-noise ratio, each PLIF image was filtered in a spatial Fourier domain. The remaining particles were removed via a threshold filter (the threshold corresponded to temperature below 18 °C). The remaining voids were interpolated by 9×9 median filter. Besides, low-pass temporal filtering was applied to compensate fluctuations of the laser intensity from pulse to pulse. Frequencies above 550 Hz were filtered for this purpose. Figure 5 demonstrates an instantaneous PLIF snapshot before and after the filtering. Besides, the PLIF data was spatially averaged to fit the spatial resolution of the PIV data.

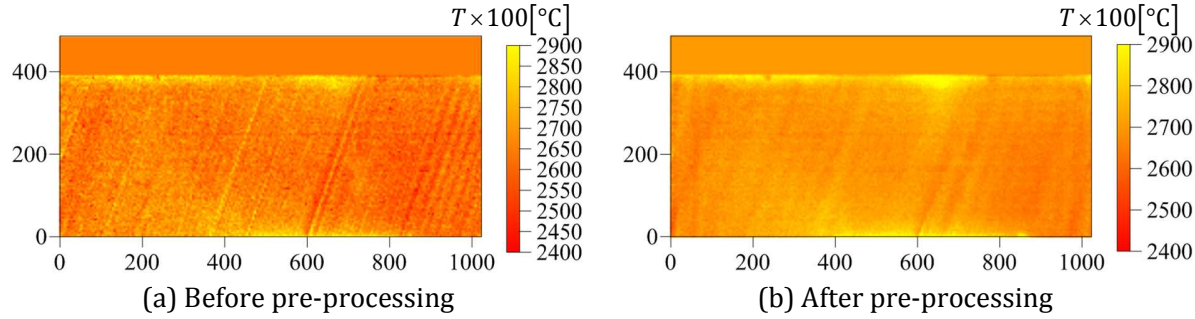

Figure 5: Effect of spatial and temporal filtering on instantaneous PLIF snapshot.

4 Results

Figure 6 shows an example of the instantaneous velocity and temperature fields, measured simultaneously. The jet flow is annular with an unsteady recirculation zone in the core. Thus, a vortex breakdown takes. Large-scale vortex structures are formed both in the inner (around the recirculation zone) and outer mixing layers. The temperature field shows that the jet is cold, whereas the highest temperatures appear near the impingement surface.

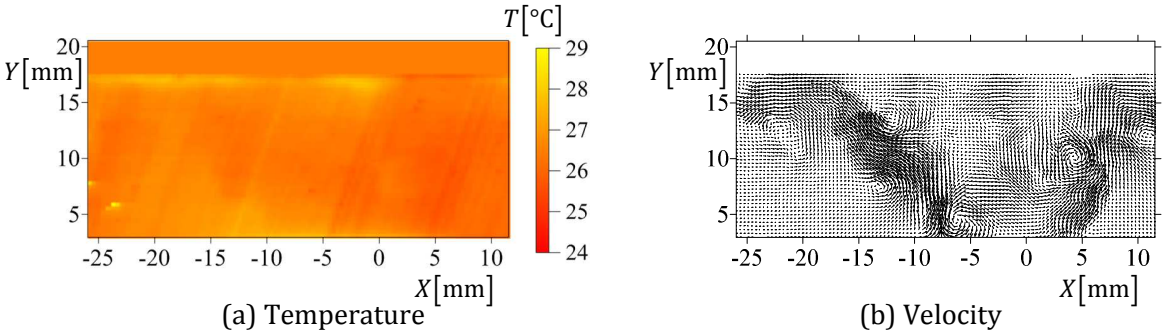

Figure 6: Instantaneous snapshots of temperature and velocity.

Figure 7 shows the time-averaged velocity and temperature fields. On average, the recirculation zone has shape of a bubble. There is a stagnation point at the surface at $X = 0$ ($Y = 1d$). According to the

PLIF data, the highest temperature for the measurement domain is near the stagnation point. Moreover, the PLIF data also shows that the laser caused noticeable heating of the nozzle.

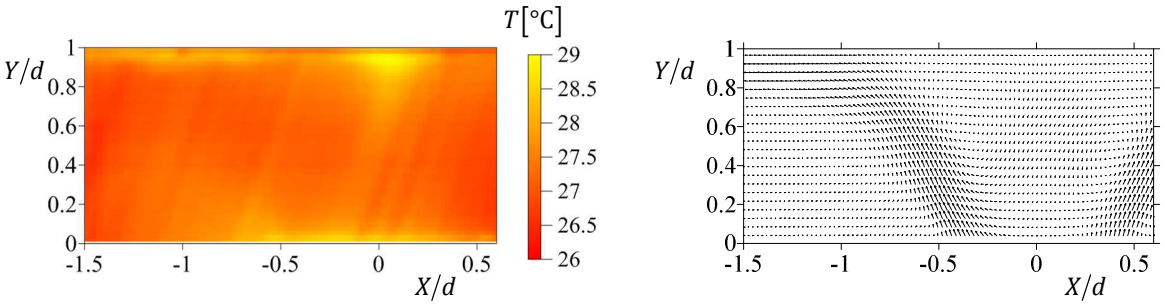

Figure 7: Time-averaged temperature and velocity fields.

Figure 8 compares temperature distributions near/at the wall obtained by two different methods. Both IR-imaging and PLIF data show a temperature peak near $X = 0$, indicating that the central recirculation zone and flow stagnation reduces heat transfer at the center. In general, shape of the PLIF data profile is similar to that of the IR imaging but the values are slightly smaller. Nevertheless, the difference between the profiles is less than 1°C.

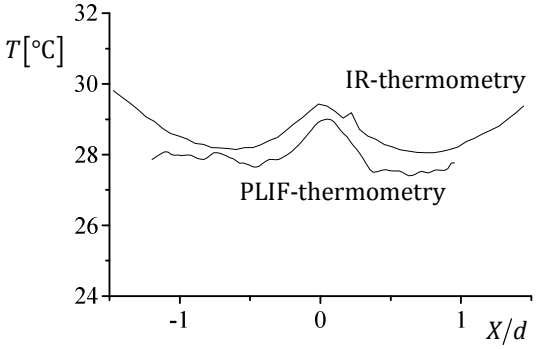

Figure 8: Time-averaged temperature of the wall (IR imaging) and liquid near the wall (PLIF data).

5 Conclusion and future work

Time-resolved stereoscopic PIV has been combined with time-resolved PLIF thermometry and high-speed IR imaging to investigate the flow dynamics in a swirling impinging jet and convective heat transfer. After spatial and temporal filtering of the PLIF data, a reliable accuracy is achieved for evaluation of the mean temperature field. The future work assumes post-processing of the instantaneous velocity and temperature snapshots by proper orthogonal decomposition to reveal coherent flow structures and their effect on the convective heat transfer.

Acknowledgements

The research is supported by the Russian Science Foundation (grant No 16-19-10566).

References

Abrantes JK and Azevedo LFA (2006) Fluid flow characteristics of a swirl jet impinging on a flat plate. In *13th International Symposium on Applications of Laser Techniques to Fluid Mechanics*, Lisbon, Portugal, June 26-29

Alekseenko SV, Bilsky AV, Dulin VM, and Markovich DM (2007) Experimental study of an impinging jet with different swirl rates. *International Journal of Heat and Fluid Flow* 28:1340–1359

Astarita T, Cardone G, Carlomagno G, and Meola C (2000) A survey on infrared thermography for convective heat transfer measurements. *Optics & Laser Technology* 32:593–610

Azevedo LFA, Almeida JA, and Duarte LGC (1997) Mass transfer to swirling impinging jets. In *4th World Conference on Experimental Heat Transfer, Fluid Mechanics and Thermodynamics*, Brussels, Belgium, June 2-6

Carlomagno GM and Cardone G (2010) Infrared thermography for convective heat transfer measurements. *Experiments in Fluids* 49:1187–1218

Gupta AK, Lilley DG, and Syred N (1984) *Swirl flows*. Abacus Press, Tunbridge Wells, Kent, England

Huang L and El-Genk MS (1998) Heat transfer and flow visualization experiments of swirling, multi-channel, and conventional impinging jets. *International Journal of Heat and Mass Transfer* 41: 583-600

Ianiro A and Cardone G (2012) Heat transfer rate and uniformity in multichannel swirling impinging jets. *Applied Thermal Engineering* 49: 89-98

Nozaki A, Igarashi Y, and Hishida K (2003) Heat transfer mechanism of a swirling impinging jet in a stagnation region. *Heat Transfer-Asian Research* 32: 663-673.

Sciacchitano A, Scarano F, and Wieneke B (2012) Multi-frame pyramid correlation for time-resolved PIV. *Experiments in Fluids* 53:1087–1105

Soloff SM, Adrian RJ, and Liu ZC (1997) Distortion compensation for generalized stereoscopic particle image velocimetry. *Measurement Science and Technology* 8:1441

Volchkov EP, Lukashov VV, and Semenov SV (1996) Heat transfer in an impact swirling jet. *Heat Transfer Research* 27: 14-24